Adaptive Sensing Schedule for Dynamic Spectrum Sharing in Time-varying Channel

Adaptive Sensing Schedule for Dynamic Spectrum Sharing in Time-varying Channel

Mengwei Sun, Xiang Wang, Chenglin Zhao, Bin Li, Y.-C.Liang, George Goussetis, Sana Salous

***Abstract*—Dynamic spectrum sharing is considered as one of the key features in the next-generation communications. In this correspondence, we investigate the dynamic tradeoff between the sensing performance and the achievable throughput, in the presence of time-varying fading (TVF) channels. We first establish a unified dynamic state-space model (DSM) to characterize the involved dynamic behaviors. On this basis, a promising dynamic sensing schedule framework is proposed, whereby the sensing duration is adaptively adjusted based on the estimated real-time TVF channel. We formulate the sensing-throughput tradeoff problem mathematically, and further show that there exists the optimal sensing duration maximizing the throughput for the secondary user (SU), which will change dynamically with channel gains. Relying on our designed recursive sensing paradigm that is able to blindly acquire varying channel gains as well as the PU states, the sensing duration can be then adjusted in line with the evolving channel gains. Numerical simulations are provided to validate our dynamic sensing schedule algorithm, which can significantly improve the SU's throughput by reconfiguring the sensing duration according to dynamic channel conditions.**

***Index Terms*—Sensing-throughput tradeoff, time-varying fading channel, dynamic sensing schedule, spectrum sensing, channel gain estimation.**

I. Introduction

By permitting dynamic spectrum sharing, cognitive radio (CR) provides a new paradigm for opportunistic access of secondary users (SUs) to licensed bands, which are allocated originally to primary users (PUs) [1]. To share the primary band harmoniously without interfering the legal PUs, the SUs should firstly monitor licensed bands within given sensing time [2], and then opportunistically emit signals in transmission slots if none of the ongoing licensed operations are detected.

One of the fundamental importance to CR networks is the tradeoff between the sensing accuracy and the SU's throughput. That is, in the context of shared access, an optimal sensing duration should be determined, by maximizing the achievable shared throughput under the constraint that the PUs are sufficiently protected against harmful interference. Such an optimization problem was firstly considered by [3]. According to [3], the optimal sensing duration exists indeed, and a periodical sensing-transmission frame structure was proposed. Thereafter, the trade-off over Nakagami fading channel was considered in [4], which focused on the effects from fading parameters on the achievable throughput. In general, previous works assume the knowledge of wireless channels to be fully available at SUs, which will become impractical in some application scenarios [5], e.g. mobile or dynamic environments. Lately, an estimation-sensing-throughput tradeoff was formulated in [6] to solve the optimization problem with imperfect link knowledge. Reference [7] investigated this problem in the presence of Rayleigh fading channel by using multi-antenna system to improve the sensing-throughput tradeoff. However, the way to deal with random fading channel is based on the *a priori* statistical probability density function (PDF). Hence, it can only characterize the instantaneous random behavior, while may fail to model the evolutions of fading channels.

In this correspondence, we focus on the effects from time-varying fading (TVF) channel to sensing-throughput tradeoff. The main contributions are summarized into three aspects. Firstly, we formulate a dynamic state-space model (DSM) which fully characterizes the spectrum sharing system in the presence of TVF channel. In our stochastic model, relying on the transfer characteristic of TVF channel, the frame period is fixed while the sensing duration changes adaptively. Secondly, the sensing-throughput tradeoff is formulated mathematically as a dynamic optimization problem under the constraint condition of predefined sensing accuracy. Based on this formulation, we prove that the optimum sensing duration is uniquely existing for identical channel gain but varies with respect to dynamic channel gain. Finally, an adaptive schedule with joint spectrum sensing algorithm is designed. Joint spectrum sensing algorithm can track the TVF channel gains and detect the PU states. Based on the real-time channel estimation, the adaptive optimal sensing duration is derived.

The paper is organized as follows. In Section II, we formulate the DSM. The traditional sensing-throughput tradeoff problem is smartly introduced in Section III. In Section IV, the adaptive sensing schedule program is formulated. Numerical results and conclusions are provided in Section V and VI.

The notations used are defined as follows. $Q(\cdot)$ denotes Q function which is the tail probability of standard normal distribution. $\mathrm{PU_T}$-$\mathrm{SU_T}$, $\mathrm{PU_T}$-$\mathrm{SU_R}$ and $\mathrm{SU_T}$-$\mathrm{SU_R}$ represent the sensing channel link from PU emitter to SU emitter, interference link from PU emitter to SU receiver and secondary link from SU emitter to SU receiver representatively. SNR_{ps} denotes the signal-to-noise ratio (SNR) of $\mathrm{PU_T}$-$\mathrm{SU_T}$ link.

M. W. Sun and George Goussetis are with the Heriot-Watt University, Edinburgh, EH14 4AS, UK (mengwei.sun@hw.ac.uk; g.goussetis@hw.ac.uk)

B. Li and C. L. Zhao are with the School of Information Science and Engineering, Beijing University of Posts and Telecommunications, Beijing 100876, China (clzhao@bupt.edu.cn; stonebupt@gmail.com).

X. Wang is with the Beijing Jianyi Corporation Limited Company.

Y.-C.Liang is with the University of Sydney.

S. Salous is with the School of Engineering and Computing Sciences, Durham University.

This work was supported by the EPSRC EP/P025129/1, National Science Foundation of China under Grants 61379016, 61471061.

II. System Model

Fig. 1 shows the frame structure designed for SU with periodic spectrum sensing. Each frame consists of one sensing slot and one data transmission slot, i.e., $T_f = T_s(n) + T_t(n)$, $n = 0, 1, \cdots$. In the sensing slot, the detection result is obtained based on the sampling signals. $M(n)$ and τ denote the sampling size and period respectively, $T_s(n) = M(n)\tau$. In this work, we design a dynamic sensing schedule scheme with considering TVF channel of PU_T-SU_T link. Specifically, the frame period is fixed while the sensing duration may change adaptively relying on the transitional behavior of fading channel. Given the sampling frequency $f_s = 1/\tau$ is generally fixed for a receiving device, then the sampling size $M(n)$ will be adjustable.

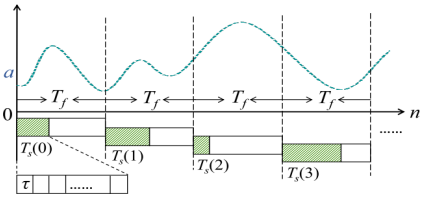

Fig. 1. Frame structure for SU with dynamic sensing duration

The discrete time DSM is formulated as:

$$\mathbf{x}(n) = \Phi(\mathbf{x}(n-1)), \tag{1}$$

$$h(n) = \Psi(h(n-1)), \tag{2}$$

$$y(n) = \Omega(\mathbf{x}(n), h(n), \mathbf{w}(n)). \tag{3}$$

In the state equation (1), $\mathbf{x}$ denotes the PU states and come into two forms: active $\mathcal{H}_1$ and dormant $\mathcal{H}_0$, the complex PSK modulated signal is considered under $\mathcal{H}_1$. The evolution behavior of PU state is characterized as a two-state Markov chain. The durations of active and dormant states are assumed exponentially distributed with mean values of α_1 and α_0, respectively [8]. Parameters α_1 and α_0 can be estimated using statistical methods based on finite samples and regarded as *a priori* information. Then, the stationary probabilities of two states can be calculated as $p(\mathcal{H}_1) = \frac{\alpha_1}{\alpha_1+\alpha_0}$ and $p(\mathcal{H}_0) = \frac{\alpha_0}{\alpha_1+\alpha_0}$. The transition probability matrix (TPM) $\mathbf{P}_s$ is time-varying but can be estimated easily with established parameters α_1 and α_0.

$$\begin{aligned}\mathbf{P_s} &= \begin{bmatrix} p_{\mathcal{H}_0\to\mathcal{H}_0} & p_{\mathcal{H}_0\to\mathcal{H}_1} \\ p_{\mathcal{H}_1\to\mathcal{H}_0} & p_{\mathcal{H}_1\to\mathcal{H}_1} \end{bmatrix}, \\ &= \frac{1}{\alpha_0+\alpha_1}\begin{bmatrix} \alpha_0+\alpha_1 e^{-(\alpha_0+\alpha_1)t} & \alpha_1-\alpha_1 e^{-(\alpha_0+\alpha_1)t} \\ \alpha_0-\alpha_0 e^{-(\alpha_0+\alpha_1)t} & \alpha_1+\alpha_0 e^{-(\alpha_0+\alpha_1)t} \end{bmatrix}.\end{aligned} \tag{4}$$

In state equation (2), $h = ae^{j\theta}$ denotes the TVF channel state of PU_T-SU_T link, with fading amplitude a and phase θ. The phase θ is uniformly distributed within the domain $[0, 2\pi)$. The amplitude a is assumed to be Rayleigh fading [9] and its statistical PDF with scale parameter σ_R^2 is:

$$f_A(a) = \frac{a}{\sigma_R^2}\exp\left(-\frac{a^2}{2\sigma_R^2}\right), \quad a > 0. \tag{5}$$

Since our study focuses on the slow-fading case, we assume the fading channel changes at a rate much slower than the PU state, i.e. the coherence time of channel $T_c \approx 1/f_D$ is greater than the frame period T_f, where f_D denotes the maximum Doppler shift. Furthermore, the channel gain is assumed to be invariant within several successive frames, i.e., $T_c = JT_f$ and J is a positive integer. To this end, we define the *transition frame* as the frame where the channel gain will possibly vary and whose indexes are $n = lJ$ $(l = 0, 1, \cdots)$.

As far as the slow-fading TVF channel is considered, the first-order finite-state Markov chain (FSMC) model is adopted owing to its effectiveness [9]. In the FSMC model, the fading amplitude is partitioned to K non-overlapping regions, i.e., $[v_0, v_1), [v_1, v_2), \cdots, [v_{K-1}, v_K)$, and each region is represented by one feasible state A_k, $A_k \in [v_k, v_{k+1})$ with the stationary probability $\pi_k \triangleq \int_{v_k}^{v_{k+1}} f_A(a)da, k = 0, 1, \ldots, K-1$. A common strategy in constructing the FSMC model is the equal partition rule, i.e., let $\pi_k = 1/K$. And the representative fading state is $A_k = \int_{v_k}^{v_{k+1}} a f_A(a)\, da/\pi_k$. The set of representative fading states is given as $\mathcal{A} = \{A_0, A_1, \cdots, A_{K-1}\}$. The amplitude $a(n) \in \mathcal{A}$ and evolves according to the first-order Markov process at the transition frames but stays the same at the remaining frames. The transitional probabilities in the TPM of the channel evolution process $\mathbf{P}_a$ relate only to the PDF of channel amplitude and states number [9], and hence can be regarded as static and established as *a priori* information.

Without losing the generality, the ED-based sensing is used and the observation in (3) conditioned on two hypotheses is:

$$y(n) = \begin{cases} \sum_{m=1}^{M(n)} |w(n,m)|^2, & \mathcal{H}_0, \\ \sum_{m=1}^{M(n)} |a(n)x(n,m) + w(n,m)|^2, & \mathcal{H}_1. \end{cases} \tag{6}$$

Here, $w(n, m)$ denotes circularly symmetric complex Gaussian (CSCG) noise case. In the following analysis, we make the following assumptions for the above DSM.

(AS1) The emitted signals are independent and identically distributed (IID) with mean zero and variance σ_x^2. The noise is IID with mean zero and variance σ_w^2. These two random processes are independent from each other and known to SU. The noise uncertainty and hardware imperfections will not be considered in our investigation [10], [11].

(AS2) As the ED detection is used, the amplitude-centric FSMC model is suitable, without considering the effects from channel phase to the observations, as shown in (6).

III. Traditional Sensing-throughput Tradeoff

In this section, the regulatory constrains for sensing-throughput tradeoff under statical channel are presented, where the sampling size is constant, i.e., $M(n) \equiv M$. The sensing performance is characterized with the probability of false alarm $p_f \triangleq p(y > \xi \mid \mathcal{H}_0)$ and the detection probability $p_d \triangleq p(y > \xi \mid \mathcal{H}_1)$. ξ is the detection threshold and is chosen to obtain a certain detection probability $\bar{p}_d$ owing to the regulatory constraints from some telecommunication standards. For instance, $\bar{p}_d$ is chosen above 0.9 in IEEE 802.22 WRAN [12].

Based on [3], the fundamental tradeoff under statical channel can be stated as an optimization problem with an overall consideration of sensing capability and achievable throughput,

$$\max_M U(M, \gamma), \tag{7}$$

$$\text{s.t.} \quad p_d(\xi, M, \gamma) \geq \bar{p}_d. \tag{8}$$

where $\gamma = a^2\sigma_x^2/\sigma_w^2$ is the value of SNR_{ps}, the achievable throughput $U(M, \gamma) = \frac{T_f - M\tau}{T_f} C_0 \left[1 - p_f(M, \gamma)\right] p(\mathcal{H}_0)$ [3]. $C_0 =$

$\log_2(1+SNR_{ss})$ where SNR_{ss} represent the SNR for the SU-SU link.

Existing methods give the optimization solution by obtaining the M corresponds to the maximum point of $U(M,\bar{\gamma})$ where $\bar{\gamma}$ is the expectation SNR. However, in practical CR networks with wireless propagations, the value of γ is commonly unknown and dynamic (e.g. due to TVF channel), and therefore, existing methods can only achieve an expected fair performance but is no longer optimal. To combat with these challenges, we further design an adaptive sensing schedule which can adjust the optimal sensing duration for every frame based on the accurate real-time estimation of γ.

IV. Adaptive Sensing Schedule

In this section, we first formulate the sensing-throughput tradeoff under TVF channel mathematically, then analyze the relation between the optimal sampling size and SNR_{ps}. Finally, the adaptive sensing schedule is illustrated.

A. Problem Formulation

Considering the dynamic $\gamma(n)$, the achievable throughput can be written as:

$$U(M,\gamma) = C_0 p(\mathcal{H}_0)\sum_{n=0}^{N-1} u(M(n),\gamma(n)), \tag{9}$$

where $u(M(n),\gamma(n))$ denotes the throughput in one frame and,

$$u(M(n),\gamma(n)) = \left[1-\frac{M(n)\tau}{T_f}\right]\left[1-p_f(M(n),\gamma(n))\right]. \tag{10}$$

The optimization problem in (7) (8) can be restated as:

$$\max_{M(n)} u(M(n),\gamma(n)), \quad n=0,1,\cdots,N-1, \tag{11}$$

$$\text{s.t.} \quad p_d(M(n),\gamma(n)) \geq \bar{p}_d. \tag{12}$$

Different from the conclusive results in [3], we can see from (10) that the achievable throughput is a *joint* function of sampling size as well as SNR_{ps}.

Theorem 1: The maximum point of $u(M(n),\gamma(n))$ for $M(n)$ is uniquely existing on one certain $\gamma(n)$ when $p_f(M(n),\gamma(n)) \leqslant 0.5$ but **sensitive to different** $\gamma(n)$.

This theorem will hold if the following two propositions can be proven.

Proposition 1: There is a unique maximum point of the $u(M(n),\gamma(n))$ within the interval $M\tau \in (0,T_f)$ with respect to one certain $\gamma(n)$.

Proposition 2: The optimal sampling size yields the highest throughput varies with respect to different $\gamma(n)$.

Proof for *Proposition 1*: For a target $\bar{p}_d$, the partial derivative of $u(M(n),\gamma(n))$ with respect to $M(n)$ can be derived as (13), where, $\beta(n) = \sqrt{2\gamma(n)+1}Q^{-1}(\bar{p}_d) + \sqrt{M(n)}\gamma(n)$ and $p_f(M(n),\gamma(n)) = Q(\beta(n))$.

$$\begin{aligned} D(M(n),\gamma(n)) &= \frac{\partial u(M(n),\gamma(n))}{\partial M(n)}, \\ &= -\frac{\tau}{T_f}\left[1-Q\left(\beta(n)\right)\right] + \frac{\gamma(n)\left[T_f - M(n)\tau\right]}{2T_f\sqrt{2\pi M(n)}}\exp\left[-\frac{\beta(n)^2}{2}\right]. \end{aligned} \tag{13}$$

As $Q(\cdot)$ is monotonic decreasing and $Q(0)=0.5$, we have:

$$\lim_{M(n)\tau\to 0} D(M(n),\gamma(n)) = +\infty, \tag{14}$$

$$\lim_{M(n)\tau\to T_f} D(M(n),\gamma(n)) < -\frac{\tau}{T_f}\left[1-Q\left(\beta(n)-\sqrt{M(n)}\gamma(n)\right)\right] < 0. \tag{15}$$

We conclude from (14) and (15) that $D(M(n),\gamma(n))$ increases when $M(n)$ is small but decreases when $M(n)$ approaches T_f/τ. Thus, there exists a maximum point of $u(M(n),\gamma(n))$ within definitional domain $M(n)\in(0,T_f/\tau)$.

As for the probability of false alarm,

$$\frac{\partial p_f(M(n),\gamma(n))}{\partial M(n)} = -\frac{\gamma(n)}{2\sqrt{2\pi M(n)}}\exp\left[-\frac{\beta(n)^2}{2}\right] < 0, \tag{16}$$

$$\begin{aligned} &\frac{\partial^2 p_f(M(n),\gamma(n))}{\partial M(n)^2}, \\ &= \frac{\gamma(n)}{4\sqrt{2\pi}M(n)}\left[\frac{1}{\sqrt{M(n)}}+\gamma(n)\beta(n)\right]\exp\left[-\frac{\beta(n)^2}{2}\right]. \end{aligned} \tag{17}$$

We can conclude from (16) that $p_f(M(n),\gamma(n))$ is decreasing with $M(n)$. Furthermore, when $\beta(n)\geqslant 0$, i.e., $p_f(M(n),\gamma(n)) \leqslant 0.5$, from (17) we have $\partial^2 p_f(M(n),\gamma(n))/\partial M(n)^2 > 0$ which means that $\partial p_f(M(n),\gamma(n))/\partial M(n)$ is monotonically increasing in $M(n)$, i.e., $p_f(M(n),\gamma(n))$ is convex. Therefore, from (13), it follows that $D(M(n),\gamma(n))$ is decreasing in $M(n)$, which further implies $u(M(n),\gamma(n))$ is concave in $M(n)$ when $p_f(M(n),\gamma(n)) \leqslant 0.5$. This indicate the maximum point of $u(M(n),\gamma(n))$ will be unique in this range.

Proof for *Proposition 2*: The mixed partial derivative of $u(M(n),\gamma(n))$ is shown in (22), which is impossible to become zero. Hence, we conclude that the optimal $M(n)$ satisfying $D(M(n),\gamma(n))=0$ will be associated with the varying $\gamma(n)$.

Note that, since the channel gain $a(n)$ evolves as a FSMC process and $a(n)\in\mathcal{A}$, we can have that $\gamma(n) = a(n)^2\sigma_x^2/\sigma_w^2$ evolves also as an FSMC process with the same TPM $\mathbf{P}_a$, and $\gamma(n)\in\mathcal{R}=\{R_0,R_1,\cdots,R_{K-1}\}$ where $R_k = A_k^2\sigma_x^2/\sigma_w^2$. Continue without changing paragraph, the reconfiguration relation between the optimal sampling size $M_k^\dagger$ and R_k can be presented as $\Delta = \left[\left\{R_0,M_0^\dagger\right\},\left\{R_1,M_1^\dagger\right\},\cdots,\left\{R_{K-1},M_{K-1}^\dagger\right\}\right]$ which should meet the condition that $D(M_k^\dagger,R_k)=0$. The key conception of our proposed adaptive sensing schedule is that the sampling size $M(n)$ of each frame will be adapted with regards to the current $\gamma(n)$, which is determined via the reconfiguration relation above, i.e. $M(n)\in\mathcal{M}=\left\{M_0^\dagger,M_1^\dagger,\cdots,M_{K-1}^\dagger\right\}$.

B. Adaptive-Joint Sensing Algorithm

In order to accomplish the dynamic reconfiguration of the sampling size, the channel gain estimation and the PU state detection need to be jointly implemented. The proposed adaptive-joint sensing algorithm is iterative and accomplished by the following three steps.

1) Sampling size determination: Inside one frame n, the SU is fed with an initial number of optimal sample size $M(n)$ which is determined based on the predictive SNR_{ps}, i.e., $\gamma(n\mid n-1)$, with the reconfiguration set Δ. As mentioned before, the SNR_{ps} related to channel state may transmit only

$$\frac{\partial^2 u(M(n),\gamma(n))}{\partial M(n)\partial\gamma(n)} = \frac{1}{\sqrt{2\pi}T_f}\exp\left[-\frac{\beta(n)^2}{2}\right]\left\{\frac{T_f - M(n)\tau}{2\sqrt{M(n)}} - \left[\frac{Q^{-1}(\bar{p}_d)}{2\sqrt{2\gamma(n)+1}} + M(n)\right]\left[\tau + \frac{T_f - M(n)\tau}{2\sqrt{M(n)}}\beta(n)\gamma(n)\right]\right\}. \quad (22)$$

in the transition frames but stay static in the remaining frames. Therefore, $\gamma(n \mid n-1)$ is obtained by:

$$\gamma(n|n-1) = \begin{cases} \arg\max\limits_{\gamma(n)\in\mathcal{R}} p\left(\gamma(n) \mid \hat{\gamma}(n-1)\right), & \text{transition}, \\ \hat{\gamma}(n-1), & \text{remaining}, \end{cases} \quad (23)$$

where the prior probability $p(\gamma(n)|\hat{\gamma}(n-1))$ is obtained based on the TPM $\mathbf{P}_a$ and the estimated SNR_{ps} of the previous frame.

The reconfigure is executed by establishing the optimal sampling size $M(n)$ as $M_k^\dagger$ if the predictive SNR_{ps} value $\gamma(n|n-1) \equiv R_k$, where $k \in \{0, 1, \cdots, K-1\}$. After reconfiguring the sampling size, the observation $y(n)$ can be obtained according to (6).

2) Channel gain estimation: According to our past investigation focus on the channel estimation in uncertain CR system, i.e., [5], the algorithm for channel estimation contains two main steps as coarse detection and channel estimation by different mechanisms.

The objective of coarse detection is to obtain a rough detection of PU state and facilitate different strategies to estimate channel gain. It is derived via maximum *a posteriori* probability (MAP) criterion with inaccurate channel state assumption $a^\dagger$ which is the minimum of channel gain set $\mathcal{A}$:

$$\mathbf{x}(n)^\dagger = \arg\max_{\mathbf{x}(n)\in\{H_0,H_1\}} p\left[\mathbf{x}(n) \mid y(n), a^\dagger\right]. \quad (23)$$

For different results of coarse detection, the channel estimations will be implemented respectively according to different mechanisms. Specifically, when $\mathbf{x}(n)^\dagger = \mathcal{H}_0$, there is little observed information that can be utilized. So, we obtain the estimation based on the prior transition property,

$$\hat{a}(n) = \begin{cases} \arg\max\limits_{a(n)\in\mathcal{A}} p\left[a(n) \mid \hat{a}(n-1)\right], & \text{transition}, \\ \hat{a}(n-1), & \text{remaining}. \end{cases} \quad (24)$$

Otherwise, when $\mathbf{x}(n)^\dagger = \mathcal{H}_1$, the joint estimation algorithm will be implemented via the MAP criterion and accumulative modification mechanism [5].

$$\hat{a}(n)^{\text{MAP}} = \arg\max_{a(n)\in\mathcal{A}} p\left[a(n) \mid \hat{a}_{pre}, \mathbf{x}(n)^\dagger, Y(n), G(n)\right]. \quad (25)$$

where $\hat{a}_{pre}$ denotes the estimated channel of the previous channel coherent time, i.e., $\hat{a}_{pre} = \hat{a}_{\lfloor nT_s/T_c \rfloor - 1}$. The accumulation observation and counter $\{Y(n), G(n)\}$ can be updated as:

$$\{Y(n), G(n)\} = \begin{cases} \{y(n), 1\}, & \text{transition}, \\ \{Y(n-1) + y(n), G(n-1) + 1\}, & \text{remaining}. \end{cases} \quad (26)$$

3) PU state Detection: Once the channel gain has been updated, the estimated SNR_{ps} can be updated as $\hat{\gamma}(n) = \hat{a}(n)^2\sigma_x^2/\sigma_w^2$. Then, the real-time threshold $\xi(n)$ is:

$$\xi(n) = \sigma_w^2\left[\sqrt{M(n)(2\hat{\gamma}(n)+1)}Q^{-1}(\bar{p}_d) + M(n)(\hat{\gamma}(n)+1)\right]. \quad (27)$$

The detection result is derived via the Neyman-Pearson (N-P) rule, i.e. $y(n) \underset{\mathcal{H}_1}{\overset{\mathcal{H}_0}{\lessgtr}} \xi(n)$. It's clear from (27) that the detection threshold is real-time and specified in every frame based on the current sampling size and estimated SNR_{ps}. Therefore, the detection result is accurate enough to guarantee the target detection probability $\bar{p}_d$.

C. Implementation

Based on the elaborations above, the schematic implementation of the new adaptive schedule is illustrated by Fig.2. The sampling size $M(n)$ in the sensing duration of current frame is adjusted firstly according to the predictive SNR_{ps} and the proposed reconfiguration relation Δ. Then, the observation signal $y(n)$ will be obtained and used for both channel estimation and PU state detection. The channel gain is estimated relying on different mechanisms. Then the real-time threshold can be updated for making the final decision on the PU state.

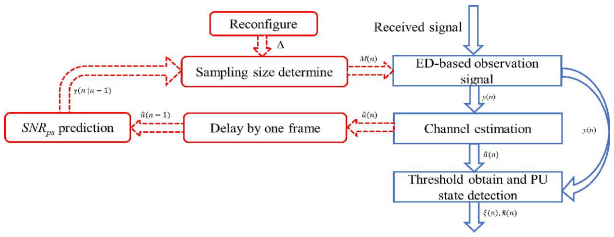

Fig. 2. Schematic implementation of the proposed adaptive sensing algorithm

V. Numerical Results and Discussions

In this section, computer simulation results and discussions are presented to evaluate the sensing-throughput tradeoff performance of proposed schedule. We choose $\alpha_0 = \alpha_1$, and hence, $p(\mathcal{H}_1) = 0.5$. $\bar{p}_d = 0.9$, $T_f = 0.1$ms, $N = 10000$, $f_D T_f = 0.01$, and $K = 8$. $SNR_{ss} = 20$dB, and hence, $C_0 = 6.6582$. The PU emitted signal is assumed to be QPSK modulated with bandwidth of 6MHz [3] and the additive noise is a zero-mean CSCG process.

We first show the joint impact of the sampling size M and the channel gain a on the SU's achievable normalized throughput which is defined as $U^\dagger = U/(NC_0)$. Fig.3 shows that $U^\dagger(M, a)$ dramatically changes with both sensing time and channel gain. Fig.4 shows that the partial derivative of throughput, i.e., $D(M, a) = \partial u(M, a)/\partial M$, is a function of M and a as well. Given that the achievable throughput $u(M, a)$ is convex which has been proven in Section IV.A, the intersection line of its partial derivative surface with the zero-flat indicates the optimal sampling size maximizing $u(M, a)$. The results of Fig.3 and Fig.4 indicate that the optimal sampling size maximizing the achievable throughput is unique for one channel gain but varies with different channel gains. Therefore, the simulated results match to the theoretical results of *Theorem 1* very well.

In Fig. 5, we then compared the maximum throughput of different configurations of the sensing duration in time-varying

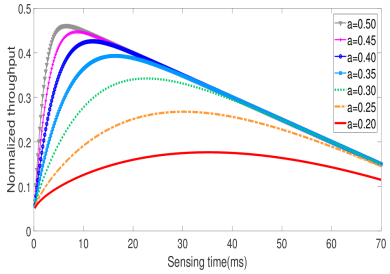

Fig. 3. SU's throughput versus the sampling size and fading channel gain

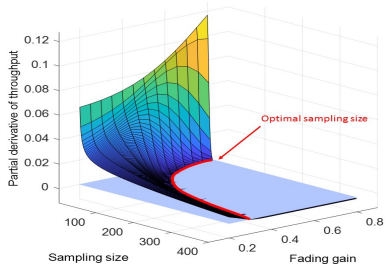

Fig. 4. Partial derivative of throughput versus the sampling size and fading channel gain

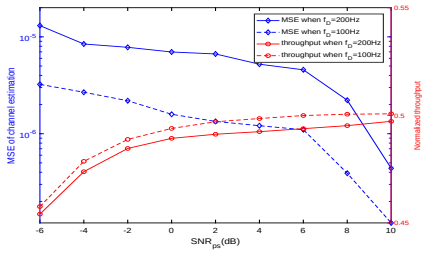

Fig. 6. Comparison of channel estimation MSE and normalized throughput under different maximize Doppler shift

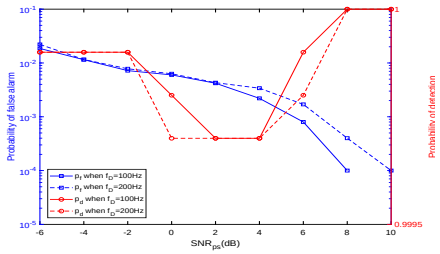

Fig. 7. Comparison of detection and false alarm probability under different maximize Doppler shift

channels. It is seen that the throughput performance of our adaptive sensing schedule, with the jointly estimated channels, may approach the ideal performance with the known channels, which also validate our designed joint channel estimation algorithm. From Fig. 5, its performance significantly outperforms the static sensing schedule schemes.

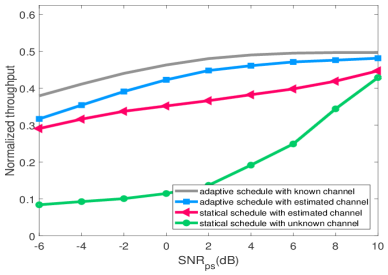

Fig. 5. Throughput performance comparison

Finally, we investigate the estimation mean square error (MSE) performance of TVF channel under different $f_D = 100Hz, 200Hz$. Moreover, the effects of channel estimation error on the detection performance as well as system throughput performance are further studied. It's clear from Fig.6 that the decrease of channel estimation error enhances the system throughput. Since accurate channel estimation can help to reduce the probability of false alarm while still guarantee the target detection probability, as shown in Fig.7.

VI. Conclusions

In this correspondence, we consider the sensing-throughput tradeoff problem in dynamic environments and design an adaptive sensing schedule scheme. Particularly, we show the optimal sensing duration is closely related with dynamic channel gains. A joint sensing algorithm with adaptive sensing duration is then proposed. Simulation results are provided to validate the designed scheme, with which the significant improvement in throughput can be attained.

References

[1] Federal Communication Commission, Spectrum Policy Task Force Report, ET Docket no.02-155, Nov. 2002.

[2] E. Axell, G. Leus, E. G. Larsson, and H. V. Poor, "Spectrum Sensing for Cognitive Radio: State-of-the-art and Recent Advances," *IEEE Signal Process. Mag.*, vol. 29, no. 3, pp. 101-116, May 2012.

[3] Y. C. Liang, Y. H. Zeng, E. C. Y. Peh, and A. T. Hoang, "Sensing-Throughput Tradeoff for Cognitive Radio Networks," *IEEE Trans. Wireless Commun.*, vol. 7, no. 4, pp. 1326-1337, Apr. 2008.

[4] M. Cardenas-Juarez, and M. Ghogho, "Spectrum Sensing and Throughput Trade-off in Cognitive Radio under Outage Constraints over Nakagami Fading," *IEEE Commun. Lett.*, vol. 15, no. 10, pp. 1110-1113, Oct. 2011.

[5] B. Li, M. W. Sun, X. F. Li, A. Nallanathan, C. L. Zhao, "Energy Detection based Spectrum Sensing for Cognitive Radios Over Time- Frequency Doubly Selective Fading Channels," *IEEE Trans. Signal Process.*, vol. 63, no. 2, pp. 402-417, Jan. 2015.

[6] A. Kaushik, S. K. Sharma, S. Chatzinotas, B. Ottersten and F. Jondral, "Performance Analysis of Interweave Cognitive Radio Systems with Imperfect Channel Knowledge over Nakagami Fading Channels," in 2016 IEEE 84th Vehicular Technology Conference (VTC-Fall), Montreal, QC, 2016, pp. 1-5.

[7] E. Soltanmohammadi, M. Orooji and M. Naraghi-Pour, "Improving the Sensing-Throughput Tradeoff for Cognitive Radios in Rayleigh Fading Channels," *IEEE Trans. Veh. Technol.*, vol. 62, no. 5, pp. 2118-2130, Jun. 2013.

[8] S. S. Kalamkar and A. Banerjee, "On the effect of primary user traffic on secondary throughput and outage probability under Rayleigh flat fading channel," in *Proc. Signal Process. Commun.*, Jul. 2014, pp. 1-6.

[9] P. Sadeghi, R. Kennedy, P. Rapajic, and R. Shams, "Finite-state Markov Modeling of Fading Channels: A Survey of Principles and Applications," *IEEE Signal Process. Mag.*, vol. 25, no. 5, pp. 57-80, Aug. 2008.

[10] S. K. Sharma, T. E. Bogale, S. Chatzinotas, B. Ottersten, L. B. Le and X. Wang, "Cognitive Radio Techniques Under Practical Imperfections: A Survey," IEEE Communications Surveys Tutorials, vol. 17, no. 4, pp. 1858-1884, Fourthquarter 2015.

[11] M. W. Sun, C. L. Zhao, S. Yan, B. Li, "A Novel Spectrum Sensing for Cognitive Radio Networks With Noise Uncertainty," *IEEE Trans. Veh. Technol.*, vol. 66, no.5, pp. 4424- 4429, May 2017.

[12] IEEE 802.22 Wireless RAN, "Functional requirements for the 802.22 WRAN standard, IEEE 802.22- 05/0007r46," Oct. 2005.